Change in the electronic states of graphite overlayers depending on thickness

A. Nagashima, H. Itoh, T. Ichinokawa, and C. Oshima
Department of Applied Physics, Waseda University, 3-4-1 Okubo, Shinjuku-ku, Tokyo 169, Japan

S. Otani
National Institute for Research in Inorganic Materials, 1-1 Namiki, Tsukuba 305, Japan
(Received 10 March 1994)

Electronic states of graphite overlayers formed on the TaC(111) surface have been investigated with the use of scanning tunneling microscopy and photoelectron spectroscopy. The graphite film grows on the substrate layer by layer. The thickness of the overlayer has been adjusted precisely to be either one or two monolayers. The physical properties of the monolayer graphite film are modified by chemical bonding at the interface. This interfacial bonding becomes weak upon the formation of the second layer of graphite, which makes the properties of the double-layer graphite film similar to those of bulk graphite.

I. INTRODUCTION

Since the discovery of fullerenes, various kinds of carbon allotropes have been studied extensively.[1-8] Particularly, the combination of the carbon allotropes with other systems has received large attention because it brings many interesting properties such as the high T_c in alkali-C_{60}. Among these allotropes, graphite is the most popular in both science and technology, and has a long history to be investigated. In relation to graphite intercalation compounds (GIC's), the interaction between the graphite basal plane and either molecules or atoms were widely clarified by many researchers.[9-14] However, little is known about the interaction between the graphite basal plane and a solid surface, especially the electronic structure at the interface.

Although the formation of monolayer graphite (MG) has so far been studied on various substrates in connection with catalysis,[15-20] this overlayer has long been considered to have almost identical properties to those of the graphite crystal because of its typical planar character. On the contrary, recent results studied by high-resolution electron-energy-loss spectroscopy have revealed a clear difference in the phonon dispersion between the MG and bulk graphite.[21-23] The phonon dispersion of the MG changes largely depending on the substrate; on chemically reactive substrates such as metal-terminated (111) surfaces of transition-metal carbides (TMC's), the MG shows large weakening of the inplane C-C bonding in comparison with the bulk graphite, while it shows strengthening of interplane bonding between the basal plane and the substrate. In contrast to the case of the reactive surfaces, such changes in the bonding of the MG have not been observed on relatively inert surfaces such as Pt(111) and the (100) surface of the TMC's. These results have indicated that the knowledge of the electronic structure at the interface is necessary for understanding the character of the graphite overlayer formed on solid surfaces.

In this experiment, we have explored the electronic properties of the graphite overlayer formed on a TaC(111) surface by using scanning tunneling microscopy (STM) and photoelectron spectroscopy (PES). The STM observation has confirmed that the film grows on the substrate layer by layer. Drastic changes in the electronic structure at the interface have been found depending on the thickness of the overlayer. The results provide insight into understanding the physical properties of the carbon-allotrope compounds.

II. EXPERIMENTAL

The experiments were done in two separate vacuum chambers. One of the chambers was equipped with a gas inlet and facilities for low-energy electron diffraction (LEED), Auger electron spectroscopy (AES), and STM (Omicron UHV-STM). The other chamber for PES measurements was equipped with a LEED optics, a hemispherical energy analyzer, an ultraviolet discharge lamp, an x-ray source, and a gas introduction system. The unpolarized He I ($h\nu=21.2$ eV) and He II (40.8 eV) resonance lines were used for angle-resolved ultraviolet photoelectron spectroscopy (ARUPS) and the characteristic x rays of Mg $K\alpha$ (1253.6 eV) were used for x-ray photoelectron spectroscopy (XPS). For the UPS and XPS measurements, the analyzer was set to have the resolution of 0.2 and 0.5 eV, respectively. Since the linewidth of the x rays is 0.7 eV, the overall energy resolution for the XPS measurements was about 0.9 eV. The base pressure in both the vacuum chamber was less than 2×10^{-8} Pa. In this experiment, we have used a TaC(111) surface as the substrate. One face of the specimen was mechanically polished to a mirror finish, and was finally cleaned in the ultra-high vacuum by flash heatings up to 1500 °C. After several heatings, the LEED pattern of the clean surface showed sharp diffraction spots in a low background, corresponding to a 1×1 atomic structure. No impurities such as oxygen or contaminated carbon were detected in both the XPS and AES spectra.

 ©1994 The American Physical Society

III. RESULTS AND DISCUSSION

A. Layer growth of graphite

The graphite layer was grown epitaxially by dissociation of ethylene gas on the substrate at high temperature. During the formation of the first monolayer of graphite, the substrate was heated at 1300 °C to make the overlayer with good crystalline quality, whereas the sample temperature was lowered to 1000 °C for the second- and third-layer formation in order to keep the carbon atoms deposited on the surface. Upon the formation of the graphite layer, an additional C 1*s* peak appears in a XPS spectrum at the binding energy of ~285 eV (as discussed later in Fig. 8), indicating the existence of graphitic carbon. The angular dependence of the peak intensity indicates that this new peak originates from the carbon atoms in the overlayer; the intensity ratio of the new peak to the substrate one increases with increasing the emission angle. Figure 1 shows a change in the intensity ratio of the C 1*s* XPS peak for the overlayer to that for the substrate as a function of ethylene exposure. For the first monolayer formation, an exposure of a few hundred langmuir (1 L = 1×10^{-6} Torr sec) was required. In comparison with the first-monolayer formation, an extremely large exposure of ~8×10^{5} L was necessary for the second-layer growth, and the growth rate of the third layer was much slower than that of the second one as shown in Fig. 1. This fact indicates that surface reactivity for ethylene dissociation is reduced at each stage of the formation of the graphite overlayer. Because of the large difference in the growth rate, the thickness of the overlayer could be precisely controlled by adjusting the exposure.

Figure 2 shows a schematic picture of an observed

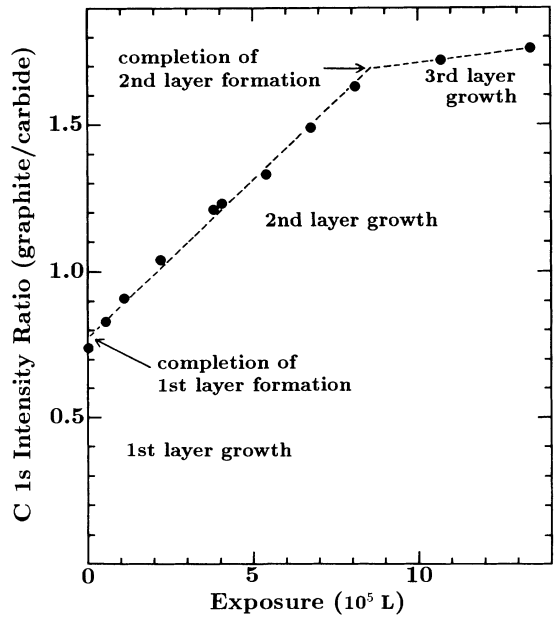

FIG. 1. The XPS intensity ratio of the graphite overlayer as a function of ethylene exposure. The vertical axis represents the intensity ratio of the C 1*s* peak for the overlayer to that for the substrate, TaC(111).

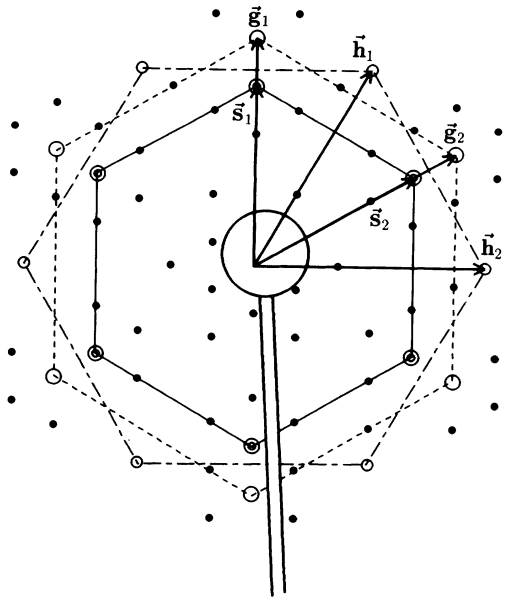

FIG. 2. Traced LEED pattern of the MG/TaC(111). The primary energy was 115 eV. $\mathbf{s}_1$ and $\mathbf{s}_2$ denote reciprocal unit vectors of the substrate. $\mathbf{g}_1$, $\mathbf{g}_2$ and $\mathbf{h}_1$, $\mathbf{h}_2$ are reciprocal unit vectors of the major and minor domain of the overlayer, respectively. Small dots represent satellite spots due to multiple diffraction.

LEED pattern for MG/TaC(111). In Fig. 2, open (double) circles indicate diffraction spots due to the overlayer (substrate). On the TaC(111) surface, the graphite overlayer has a two-domain structure. One of them has the reciprocal unit vectors $\mathbf{g}_i$ parallel to those of the substrate ($\mathbf{s}_i$), and the other has the reciprocal vectors ($\mathbf{h}_i$) rotated from $\mathbf{g}_i$ by 30°. The former domain is dominant in comparison with the latter one. Any other spots shown by small dots come from the multiple diffraction; they are located at the positions where the wave vector parallel to the surface $\mathbf{q}_{\parallel}$ satisfies the following formula: $\mathbf{q}_{\parallel}=(l_1\mathbf{g}_1+l_2\mathbf{g}_2)+(m_1\mathbf{s}_1+m_2\mathbf{s}_2)$. Here, l_1, l_2, m_1, and m_2 are integers.

After the formation of the second monolayer of graphite, the substrate spots became much weaker and only one domain with $\mathbf{g}_i$ was prominent. The lattice constant of the overlayer estimated from the LEED pattern has decreased from 2.49±0.01 Å for the MG to 2.47±0.01 Å for the double-layer graphite (DG), which is close to the bulk value, 2.46 Å. As is discussed later, this change is related to the weakening of chemical bonding at the interface.

Figure 3 shows the STM image for the TaC(111) surface exposed to the ethylene gas at about 1×10^{4} L at the sample temperature of 1000 °C. The image of the empty states was taken at the bias voltage of 2.4 V and the tunneling current of 0.08 nA. The dark area in the lower right of Fig. 3 represents the lower terrace. The surface is covered with the MG almost entirely except the area in the vicinity of the step edge, where the second graphite

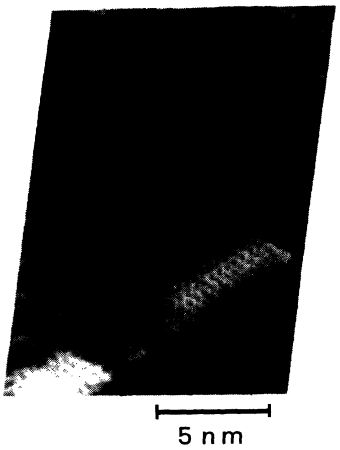

FIG. 3. The STM image of the graphite-covered TaC(111) surface taken at the bias voltage of 2.4 V and the tunneling current of 0.08 nA. The dark area in the lower right represents the lower terrace.

layer is observed. This might be a consequence of the fact that the step edge is more reactive for ethylene dissociation than the center of the terrace. The STM image of the MG-covered surface shows the moirélike pattern, which is formed by overlapping the two periodicities; one is for the overlayer and the other is for the substrate. This fact suggests that the electronic structure of the MG is modulated by the interaction with the substrate. A similar moirélike pattern has been also observed for other graphite-covered surfaces such as TiC(111) and Pt(111).[24,25] In contrast to this, the STM image for the DG shows only one kind of corrugation with the periodicity of 2.5 Å, corresponding to the lattice constant of graphite. This fact indicates that the modulation of the electronic structure in the DG is much smaller than that in the MG.

B. Valence-band structure

Figures 4(a) and 4(b) show typical ARUPS spectra of the MG/TaC(111) obtained for the $\bar{\Gamma}\bar{K}$ direction of the two-dimensional Brillouin zone (i.e., parallel to $\mathbf{g}_1+\mathbf{g}_2$) excited by He I and He II resonance lines, respectively. The emission angle referred to the surface normal is denoted for each spectrum. In Fig. 4(a), we observed almost dispersionless peaks located at the binding energy of ~ 5 eV. Since these peaks have been also observed for the clean TaC(111) surface, they are ascribed to the emission from the substrate. With the use of He II, such dispersionless peaks became small owing to the shorter mean-free path of the photoelectrons.

In Figs. 4(a) and 4(b), several peaks exhibit large energy dispersion. Since none of them have been observed for the clean substrate, they are all related to the electronic states either in the MG or at the interface. The series of peaks located at 0–1 eV show a *metallic* feature of the overlayer; the binding energies of these peaks cross the Fermi level (E_F), which is a marked contrast to the semimetallic character of the bulk graphite. In addition, the π peak splits into two at ~ 6 eV below E_F at the emission angle of 24° in Fig. 4(b), which indicates hybridization of the π orbitals with d orbitals of the substrate.

In Fig. 5, we plotted the binding energies (E_B) of the observed peaks in the ARUPS spectra of the MG/TaC(111) versus the wave vector parallel to the surface ($k_\parallel$) obtained by using the following formula:

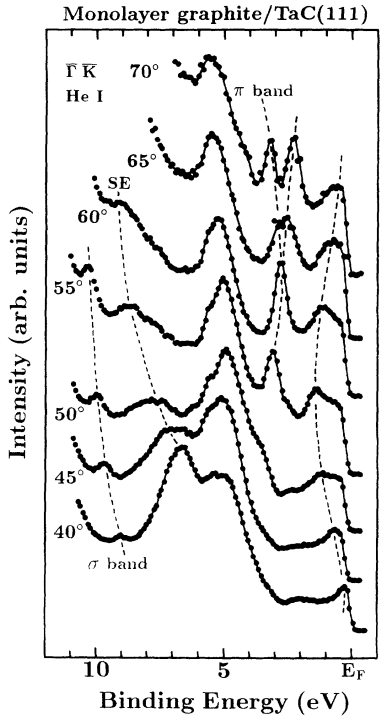

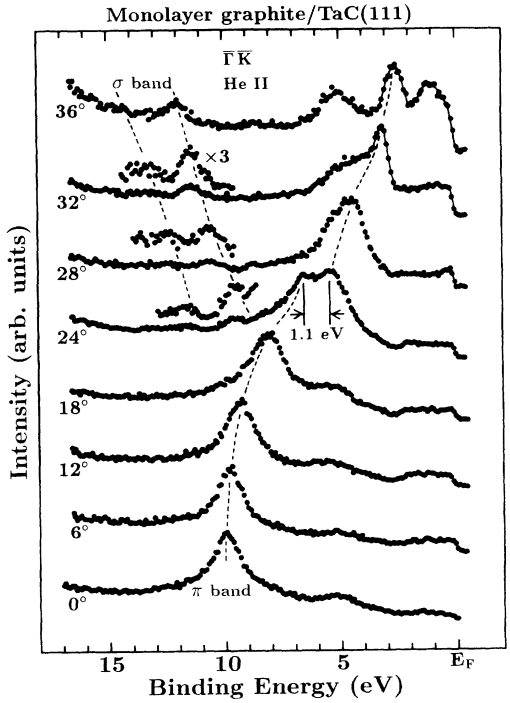

FIG. 4. Typical ARUPS spectra of the MG/TaC(111) excited by (a) He I and (b) He II, respectively. The polar angle of emitted electrons is denoted for each spectrum. "SE" is an abbreviation for "secondary electron peak."

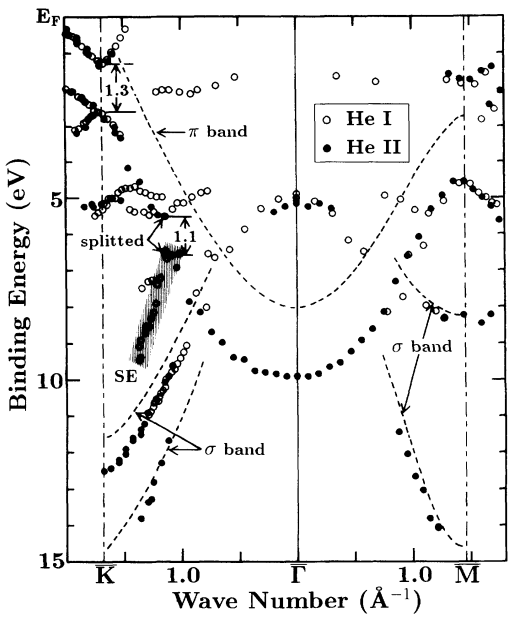

FIG. 5. Experimental band structure of the MG/TaC(111). Open (filled) circles denote the data obtained with He I (He II) resonance line. The experimental dispersion of the bulk graphite (Ref. 26) is also indicated by broken curves for comparison. SE is an abbreviation for secondary electron peak.

$$k_{\parallel}=[2m(h\nu-\phi-E_B)]^{1/2}\sin\theta\ , \tag{1}$$

where m is the rest mass of an electron, $h\nu$ the photon energy for excitation, ϕ the work function of the MG (3.7 eV, determined in the present work), and θ the emission angle. Open (solid) circles represent the data obtained with the He I (He II) resonance line. The corresponding energy bands of the graphite crystal are also indicated by broken curves.[26]

Because of the dispersive nature along the c axis, the dispersion curve of the π band in the bulk graphite obtained with a certain photon energy is different from that measured with the other photon energy.[26] For the graphite overlayer, on the other hand, all the dispersion curves measured with He II have agreed perfectly with those obtained with He I. This is the clear experimental evidence for the two-dimensional nature of the electronic structure of the MG, which is also in good accordance with the two-dimensional character of plasmons excited in this layer reported previously.[27,28]

The observed band structure of the MG in Fig. 5 is different from the bulk one shown by the broken curves. In the bulk, the π band reaches E_F at the K point of the Brillouin zone and connects with the bottom of the π^* band there.[29] In contrast, the π band in the MG possesses one energy gap at 2.6 eV below E_F at the $\bar{K}$ point, and it has another gap at around 6 eV below E_F on the $\bar{\Gamma}\bar{K}$ symmetry axis. The appearance of the two gaps of 1.3 and 1.1 eV signifies that the π (or π^*) orbitals hybridize with the d orbitals of the substrate. To our knowledge, the hybridization has never been observed in the alkali-metal GIC's.[10] In comparison with the π band, the σ bands exhibit smooth curves, which are located at almost the same energy position as the bulk graphite. They indicate clearly that the orbital hybridization takes place mainly between the π (π^*) orbitals of the overlayer and the d orbitals of the substrate.

In Fig. 5, there is one branch showing a large dispersion in the energy region of 6–10 eV along the $\bar{\Gamma}\bar{K}$, which is assigned to be the secondary electron peak for the following reasons. (1) It was observed only with He I. (2) Since this branch has been also observed for the MG on the other substrates, TiC(111) and Ni(111), it is not ascribed to the photoelectrons emitted from the substrate. (3) There are no corresponding branches in the *valence*-band structure of both the graphite crystal and the MG. (4) The observed energies relative to E_F is very similar to those of a conduction band in bulk graphite observed by secondary electron emission spectroscopy.[30]

Figures 6(a) and 6(b) show typical ARUPS spectra of the DG/TaC(111) system measured along the $\bar{\Gamma}\bar{K}$ symmetry axis parallel to the $\mathbf{g}_1+\mathbf{g}_2$ direction. For the DG, the signals from the substrate are weak in the UPS spectra excited by He I. Because of the double-domain structure of the overlayer, the ARUPS spectra are composed of the signals from both the major and minor domains. Therefore, as shown in Fig. 6, the π peak splits into two with the increase of the emission angle. These two peaks exhibit the energy dispersion along the $\bar{\Gamma}\bar{K}$ and $\bar{\Gamma}\bar{M}$ symmetry axes. We have assigned the two branches by the shape of the dispersion curves expected from the bulk one; the upward dispersion of the curve along the $\bar{\Gamma}\bar{K}$ ($\bar{\Gamma}\bar{M}$) changes to the downward one at the $\bar{K}$($\bar{M}$) point, where the wave number parallel to the surface $k_{\parallel}$ is 1.68 (1.46) Å^{-1}. It should be remarked that near the edge of the Brillouin zone, the photoionization cross section of the π band for the $\bar{\Gamma}\bar{M}$ is much larger than that for the $\bar{\Gamma}\bar{K}$. Although the LEED spots for the minor domain of $\mathbf{h}_i$ were much weaker than those for the major one of $\mathbf{g}_i$, the intensity of the π peak from the minor domain (denoted by $\bar{\Gamma}\bar{M}$ in Fig. 6) were comparable to that from the major one. On the other hand, in the spectra measured in the $\mathbf{g}_1$ direction which corresponds to the $\bar{\Gamma}\bar{K}$ direction of the minor domain, no π peak from the minor domain was observed.

Figure 7 shows the bands structure of the DG. As the thickness of the graphite overlayer increases from one to two monolayers, the electronic structure becomes close to the bulk one; the energy of the π band at the $\bar{K}$ point approaches E_F, and the band gap at the $\bar{K}$ point decreases. However, there remains a small gap. In addition, the dispersion curves of the σ bands are in perfect agreement with the bulk ones. These results are consistent with the observed work functions; i.e., while the work function of the MG, 3.7±0.1 eV, is considerably smaller than that of the graphite crystal (4.6±0.1 eV), the DG has the closer value (4.2±0.1 eV). Again, there remains a small difference between the DG and the graphite crystal.

Here, we summarize the results of the ARUPS experiment.

(1) The electronic structures of the MG and DG are different from the bulk one. The difference is much larger in the case of the MG than that of the DG.

(2) The modulation occurs for the π band in both the MG and DG, while the discrepancy of the σ bands is much smaller.

(3) In comparison with the case of the MG, the electronic structure of the DG is much similar to the bulk one. This tendency also appears in the work function, surface reactivity, and the STM image.

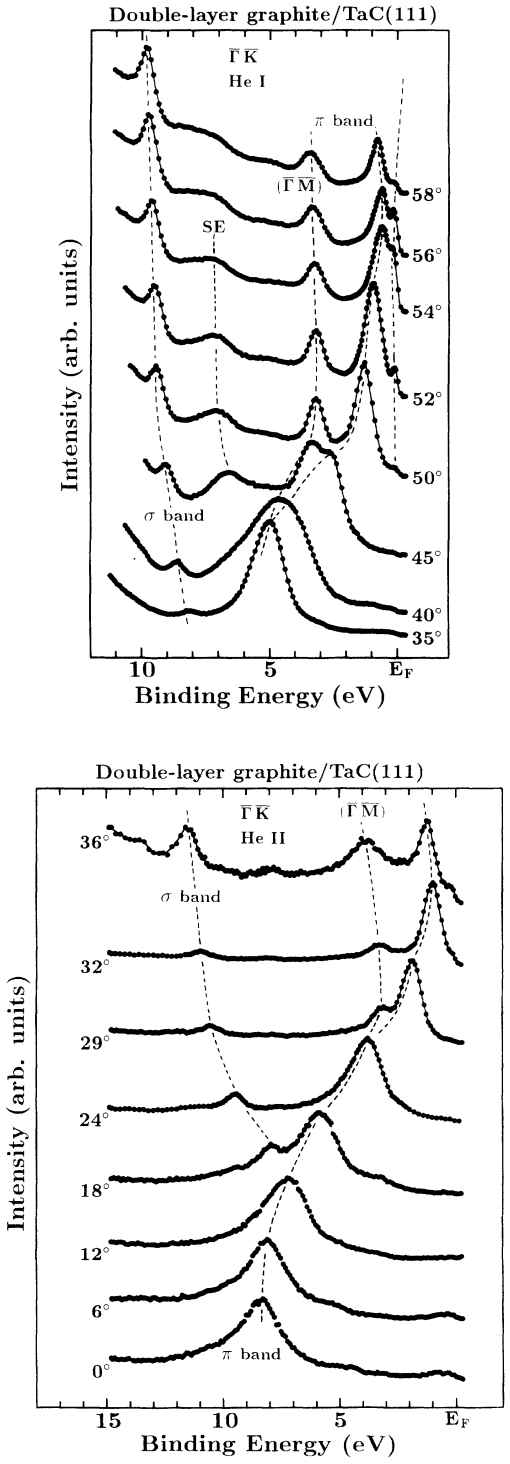

FIG. 6. Typical ARUPS spectra of the DG/TaC(111) excited by (a) He I and (b) He II, respectively.

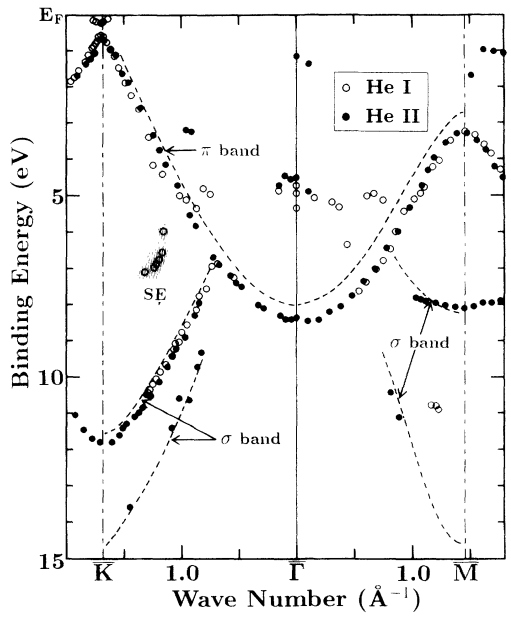

FIG. 7. Experimental band structure of the DG/TaC(111).

(4) The existence of the energy gaps in the π branch manifests the hybridization between the π (π^*) orbitals and the d orbitals of the Ta atoms. The small gap in the DG suggests that the orbital hybridization becomes weak with the change in the thickness from mono to double layers.

Recently, the hybridization of the MG has been also discussed by Kobayashi *et al.*, who calculated the electronic states of the MG formed on a Ti-terminated TiC(111) surface.[31] The physical properties of the MG is similar to those of the MG on the TaC(111) discussed in this paper. Their energy band calculations are in good agreement with our experimental dispersion curves of the MG/TiC(111).[32] On the basis of the calculations, they have pointed out two features of the electronic states in the MG/TiC(111). First, the electron transfer from the substrate to the graphite layer is little; at the largest, 0.01 electrons were estimated for each C atom. This is consistent with the small shift of the σ bands against E_F observed experimentally. Second, the hybridization of the π and π^* orbitals with the d orbitals produces the covalent bonding and causes the energy gaps in the π branch. The covalent bonding is stronger than the van der Waals bonding in the graphite crystal, and it weakens the inplane C-C bonding in the graphite layer with donation of electrons from the π states and back donation into the π^* states. In other words, the bond weakening is caused by the transfer of electrons from the π orbitals to the π^* (antibonding π) orbitals, of which the energies are lowered by the interaction with the substrate. This process is analogous to the mechanism of C-O bond weakening in CO chemisorbed on transition-metal surfaces.[33] These results are in good accordance with the observed various properties of the MG.[28,32]

Since the unit cell of the bulk graphite consists of two basal planes, overlapping of the π orbitals in the neigh-

boring planes leads to the splitting of the π band.[29] As for the DG in this experiment, however, we have observed only one π branch. There are two possible explanations for this phenomenon. First, the distance between the two atomic layers is so large that the small splitting cannot be resolved. Second, for the bulk graphite, the shallower (deeper) branch of the π band is of the antibonding (bonding) state, and appears as a prominent (faint) peak in the ARUPS spectra.[26] It implies different cross sections for photoionization. In the DG, the difference in the cross section presumably becomes large because of the better crystalline quality than that of the graphite crystal,[35] so that the deeper branch is invisible. The latter explanation seems to be more reasonable as discussed later.

C. Carbon 1s core-level state

Figure 8 shows the XPS spectra in the C 1s energy regions for various graphite and the clean TaC substrate. The left side of Fig. 8 presents the original spectra for the DG, MG, and the clean substrate, and the right side of the figure shows the difference spectra for the graphite overlayers and the original one for the bulk graphite. As for the difference spectra, the substrate peak is subtracted by adjusting the intensity of the spectrum for the clean substrate, and, therefore, the overlayer peaks located at ~285 eV are compared straightforward to the bulk graphite peak. Roughly speaking, the binding energies of the overlayer peaks are very close to the bulk one, while the substrate peak are shifted to the lower binding energy because of the electron transfer from the Ta atoms to the C atoms in the TaC crystal.[36]

From the energy width of these peaks, interesting pictures about the chemical bondings at the interface are deduced. It should be emphasized that the peak width of the DG is smaller than that of the MG formed on the same TaC(111) surface. Before discussing the reason for this phenomenon, we should first interpret another phenomenon related to it; namely, the MG on the (100) surface has the smallest full width at half maximum (FWHM) of 1.1 eV, whereas the largest one of 1.5 eV is observed for the MG/TaC(111). In the MG on the TaC(100), the electronic structure is much closer to the bulk one in comparison with that of the MG/TaC(111); this tendency is observed in the dispersion curve of the π band, the work function, the lattice constant, and the phonon frequencies.[21,28] These results indicate that the MG is coupled with the (111) surface more strongly than the (100) surface. Figure 9 presents schematic pictures of chemical bonding of the overlayer with the substrate. As shown in Fig. 9(a), the positions of the neighboring carbon atoms in the overlayer are not identical with each other because of the incommensurate relation with both the (111) and (100) surfaces. Therefore, many different bondings due to the relatively strong hybridization produce different electron distributions around the carbon atoms, causing the differences in the initial-state energy (chemical shift) and the screening effects for the corehole (relaxation shift or lifetime broadening). It is presumably the origin of the broad peak of the MG on the (111) surface. The broad peak of the graphite crystal in Fig. 8 is ascribed to the poor crystalline quality due to the defects such as misstacking of the basal planes, corrugation, and step, because we saw the ringlike diffraction spots with a high background in the LEED pattern of the graphite crystal.

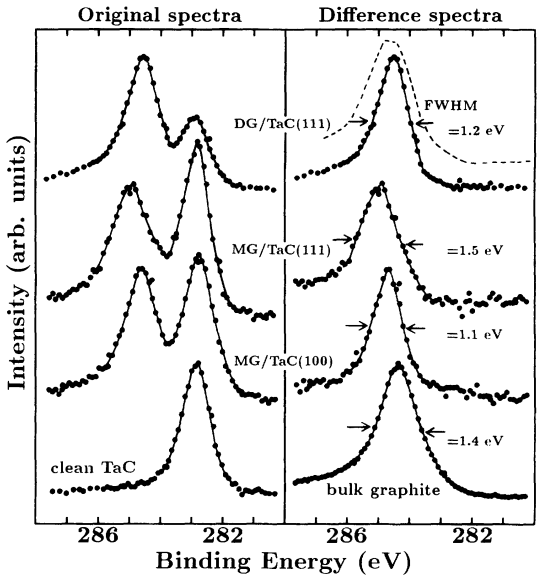

FIG. 8. C 1s region of XPS spectra. The left side of the figure shows the original XPS spectra for the DG, MG, and the clean TaC(111) substrate. The right side of the figure shows the difference spectra of the graphite overlayers where the C 1s peak of the substrate is subtracted. The spectrum of the graphite crystal is also indicated. The broken curve expresses a hypothetical spectrum calculated by superposing the two spectra of the graphite and MG/TaC(111).

Next, the peak width of the DG in Fig. 8 is discussed. Because of the large mean free path of the x-ray photoelectrons, the spectrum of the DG should be considered to consist of signals not only from the second layer of graphite but also from the first layer. In view of the fact that the basal planes in the bulk graphite are weakly bonded by van der Waals forces, it may well be supposed that the formation of the second graphite layer does not influence the interfacial bonding between the first layer and the substrate as shown in Fig. 9(b). If this expectation was valid, the spectrum of the DG would be very broad like the broken curve in Fig. 8; it was calculated by superposing the spectrum of the bulk graphite to that of the MG/TaC(111). However, the result in Fig. 8 shows that the C 1s peak of the graphite overlayer becomes narrow by the second layer growth. This fact strongly suggests that the formation of the second layer makes all the carbon atoms in the two layers have the similar states. From the above discussions together with the fact that the lattice constant of the DG is closer to the bulk one than that of the MG, we conclude that the bulklike van der Waals bondings are produced between the two basal planes in the DG, and the strength of the interfacial bonding becomes weak as is illustrated in Fig. 9(c). In other words, it could be inferred that the interplanar

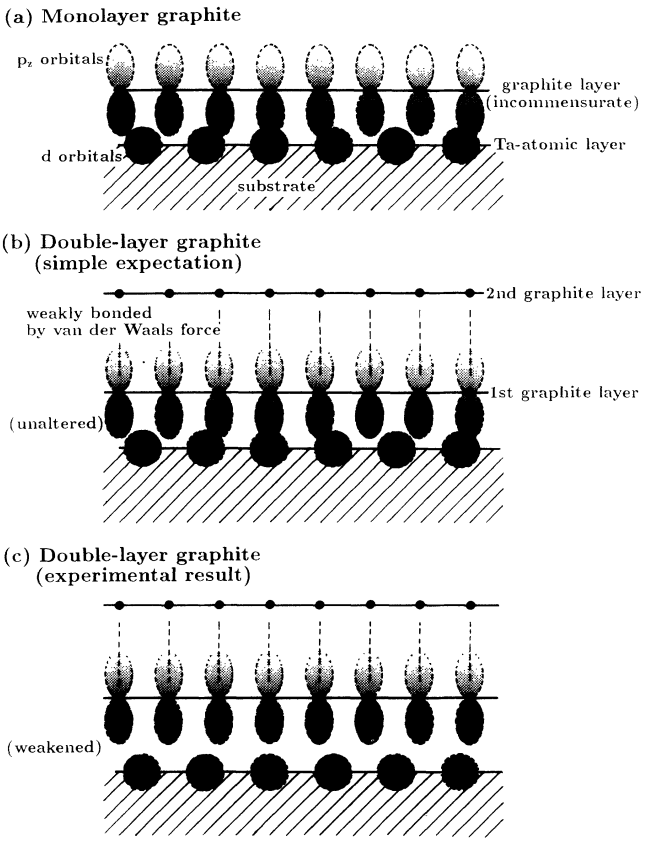

FIG. 9. Schematic pictures of the interfacial bondings. (a) Incommensurate relation of the MG with the substrate introduces many different chemical bondings at the interface. (b) Incorrect expectation; the interfacial bonding in the DG might be almost identical to those in the MG because the basal planes of the DG are weakly bonded by van der Waals force. (c) Present conclusion; the formation of the second graphite layer reduces the strength of the interfacial bondings.

bonding with commensurate relation contribute to the cohesive energy more largely than those with the incommensurate relation.

In the previous paragraph, we have discussed the two possible reasons why only one π branch was observed in the DG; one is the degeneracy of the π bands and another one is the difference in photoionization cross section. At present, we have no experimental data for the interplanar spacing in the DG. However, the present XPS result concerning the energy width shows that the two basal planes of the DG do interact, which results in the reduction of the interfacial bondings. Accordingly, we should suppose the latter explanation more feasible.

IV. CONCLUSIONS

By using STM, ARUPS, and XPS, we have investigated graphite overlayers with a thickness of one or two monolayer(s). The graphite film grows on the TaC(111) surface layer by layer. Owing to the hybridization of the π orbitals with the d orbitals of the substrate, the electronic states of the MG differ largely from those of bulk graphite. Despite the typical planar character of graphite, the orbital hybridization between the overlayer and the substrate changes depending on the thickness of the overlayer; the interfacial bonding becomes weak upon the formation of the second graphite layer. Consequently, the electronic properties of the DG are very similar to the bulk ones although there still remains the clear difference in the work function and the dispersion of the π band. We hope that the present work may provide an impetus to advanced theoretical and experimental studies of the interfacial bonding.

ACKNOWLEDGMENT

One of the authors (A.N.) was supported by JSPS.

[1]W. Krätschmer, L. D. Lamb, K. Fostiropoulos, and D. R. Huffman, Nature **347**, 354 (1990).

[2]R. C. Haddon, A. F. Hebard, M. J. Rosseinsky, D. W. Murphy, S. J. Duclos, K. B. Lyons, B. Miller, J. M. Rosamilia, R. M. Fleming, A. R. Kortan, S. H. Glarum, A. V. Makhija, A. J. Miller, R. H. Eick, S. M. Zahurak, R. Tycko, G. Dabbagh, and F. A. Theil, Nature **350**, 320 (1991).

[3]S. Saito and A. Oshiyama, Phys. Rev. Lett. **66**, 2637 (1991).

[4]P. J. Benning, F. Stepniak, D. M. Poirier, J. L. Martins, J. H. Weaver, L. P. F. Chibante, and R. E. Smalley, Phys. Rev. B **40**, 13 843 (1993).

[5]S. Iijima, Nature **354**, 56 (1991); S. Iijima, *ibid.* **363**, 603 (1993); D. S. Bethune, C. H. Kiang, M. S. de Vries, G. Gorman, R. Savoy, J. Vazquez, and R. Beyers, *ibid.* **363**, 605 (1993).

[6]N. Hamada, S. Sawada, and A. Oshiyama, Phys. Rev. Lett. **68**, 1579 (1992); J. W. Mintmire, B. I. Duniap, and C. T. White, *ibid.* **68**, 631 (1992).

[7]K. Kobayashi, Phys. Rev. B **48**, 1757 (1993).

[8]S. Ihara, S. Itoh, and J. Kitakami, Phys. Rev. B **47**, 12 908 (1993).

[9]For a review see, M. S. Dresselhaus and G. Dresselhaus, Adv. Phys. **30**, 139 (1981).

[10]N. A. Holzwarth, S. Rabii, and L. A. Gieifalco, Phys. Rev. B **18**, 5190 (1978); W. Eberhardt, I. T. McGovern, E. W. Plummer, and J. E. Fisher, Phys. Rev. Lett. **44**, 200 (1980); T. Takahashi, N. Gunasekara, T. Sagawa, and H. Suematsu, J. Phys. Soc. Jpn. **55**, 3498 (1986).

[11]D. E. Nixon and G. S. Parry, J. Phys. C **2**, 1732 (1969); D. Guérard, C. Zeller, and A. Hérold, C. R. Acad. Sci. Paris Ser. C **238**, 437 (1976).

[12]C. T. Chan, W. A. Kamitakahara, K. M. Ho, and P. C. Eklund, Phys. Rev. Lett. **58**, 528 (1987).

[13]Z. Y. Li, K. M. Hock, and R. E. Palmer, Phys. Rev. Lett. **67**, 1562 (1991).

[14]H. Ishida and R. E. Palmer, Phys. Rev. B **46**, 15 484 (1992); F. Ancilotto and F. Toigo, *ibid.* **47**, 13 713 (1993).

[15]H. Zi-pu, D. F. Ogletree, M. A. Van Hove, and G. A. Somorjai, Surf. Sci. **180**, 433 (1987).

[16]R. Rosei, S. Modesti, F. Sette, C. Quaresima, A. Savoia, and P. Perfetti, Phys. Rev. B **29**, 3416 (1984); L. Papagno and L. S. Caputi, *ibid.* **29**, 1483 (1984).

[17]N. R. Gall', S. N. Mikhoilov, E. V. Rut'kov, and A. Ya. Ton-

tegode, Sov. Phys. Solid State **27**, 1410 (1985).
[18]E. V. Rut'kov and A. Y. Tontegonde, Surf. Sci. **161**, 373 (1985).
[19]C. Oshima, E. Bannai, T. Tanaka, and S. Kawai, Jpn. J. Appl. Phys. **16**, 965 (1977).
[20]P. M. Stefan, M. L. Shek, I. Lindau, W. E. Spicer, L. I. Johansson, F. Herman, R. V. Kasowski, and G. Brogen, Phys. Rev. B **29**, 5423 (1984).
[21]T. Aizawa, R. Souda, S. Otani, Y. Ishizaw, and C. Oshima, Phys. Rev. Lett. **64**, 768 (1990); Phys. Rev. B **42**, 11 469 (1990).
[22]T. Aizawa, R. Souda, Y. Ishizaw, H. Hirano, T. Yamada, K. Tanaka, and C. Oshima, Surf. Sci. **237**, 194 (1990).
[23]T. Aizawa, Y. Hwang, W. Hayami, R. Souda, S. Otani, and Y. Ishizaw, Surf. Sci. **260**, 311 (1992).
[24]H. Itoh, T. Ichinose, C. Oshima, T. Ichinokawa, Surf. Sci. Lett. **254**, L437 (1991).
[25]T. A. Land, T. Michely, R. J. Behm, J. C. Hemminger, and G. Comsa, Surf. Sci. **264**, 261 (1992).
[26]T. Takahashi, H. Tokailin, and T. Sagawa, Phys. Rev. B **32**, 8317 (1985).
[27]A. Nagashima, K. Nuka, H. Itoh, T. Ichinokawa, C. Oshima, S. Otani, and Y. Ishizawa, Solid State Commun. **83** (1992).
[28]A. Nagashima, K. Nuka, K. Satoh, H. Itoh, T. Ichinokawa, C. Oshima, and S. Otani, Surf. Sci. **287/288** (1993).
[29]R. C. Tatar and S. Rabi, Phys. Rev. B **25**, 4126 (1982).
[30]F. Maeda, T. Takahashi, H. Ousawa, S. Suzuki, and H. Suematsu, Phys. Rev. B **37**, 4482 (1988).
[31]K. Kobayashi, M. Souzu, S. Isshiki, and M. Tsukada, Appl. Surf. Sci. **60/61**, 443 (1992).
[32]A. Nagashima, K. Nuka, K. Sato, H. Itoh, T. Ichinokawa, C. Oshima, and S. Otani, Surf. Sci. **291**, 93 (1993).
[33]G. Blyholder, J. Phys. Chem. **68**, 2772 (1964); G. Doyen and G. Ertl, Surf. Sci. **43**, 197 (1974).
[34]C. Oshima, T. Aizawa, R. Souda, Y. Ishizawa, and Y. Sumiyoshi, Solid State Commun. **65**, 1601 (1988).
[35]For instance, because of the selection rule for the electron scattering, two of the six modes for the surface phonons in the MG are invisible by using electron energy loss spectroscopy (Ref. 21), while all the modes in the bulk graphite have been observed with the same method (Ref. 34).
[36]H. Ihara (unpublished).

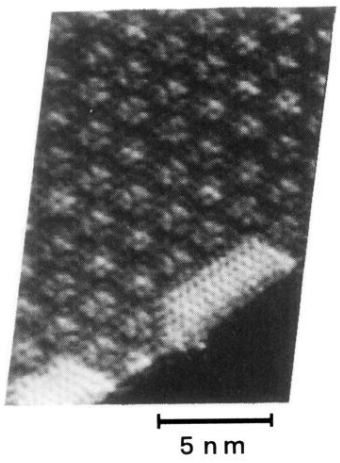

FIG. 3. The STM image of the graphite-covered TaC(111) surface taken at the bias voltage of 2.4 V and the tunneling current of 0.08 nA. The dark area in the lower right represents the lower terrace.

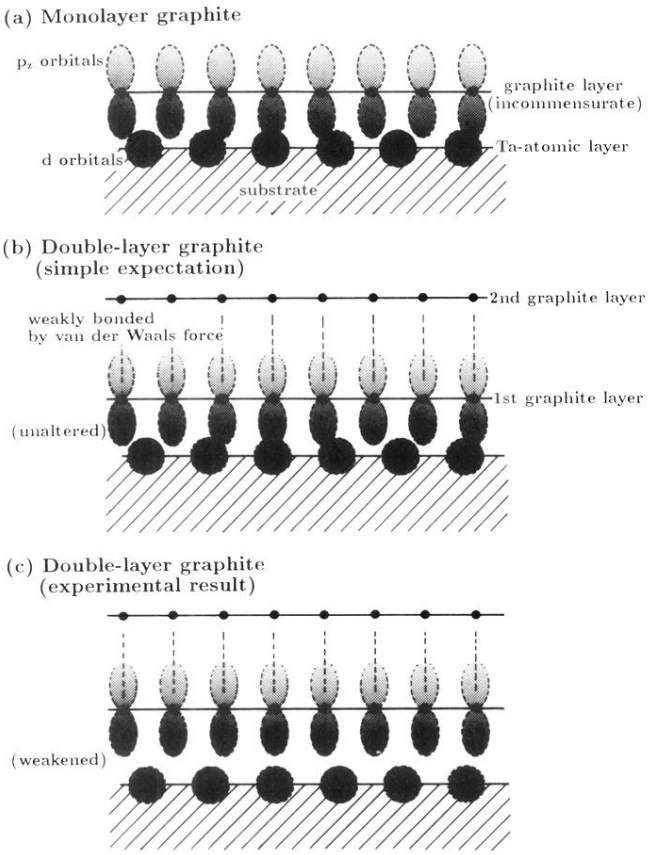

FIG. 9. Schematic pictures of the interfacial bondings. (a) Incommensurate relation of the MG with the substrate introduces many different chemical bondings at the interface. (b) Incorrect expectation; the interfacial bonding in the DG might be almost identical to those in the MG because the basal planes of the DG are weakly bonded by van der Waals force. (c) Present conclusion; the formation of the second graphite layer reduces the strength of the interfacial bondings.